Journal of the Korean Society of Marine Engineering, Vol. 36, No. 3, pp. 358~367, 2012
(ISSN 2234-8352(Online) / ISSN 2234-7925(Print)) http://dx.doi.org/10.5916/jkosme.2012.36.3.358

An Evaluation for Predicting the Far Wake of Tidal Turbines Positioned in Array at Different Longitudinal Spaces

C. J. Yang† · A. D. Hoang[1] · Y. H. Lee[2]

(Received December 15, 2011; Revised February 12, 2012; Accepted April 5, 2012)

Abstract : A study on tidal turbine using CFD simulation has been an economical and reliable method. However, large flow fields with multi-turbine arrays require high computer performance. Actuator disc theory therefore is widely applied. Actuator disc is the concept that imitates actual turbine by means of an energy absorption disc which has the same dimension and characteristics. Turbines installed in array may have disturbance effects on one another. Thus, the subject of this study is to analyze the far wake of these tidal turbines and compare to single turbine case. The main objects are to analyze two turbines positioned longitudinally at different spaces.

Key words : Tidal, Turbine, CFX, Renewable, Sustainable, Energy.

Nomenclature

- a : induction factor
- T : torque (N)
- P : pressure (Pa)
- U_o : inflow velocity (m/s)
- U_d : water velocity at disc (m/s)
- C_T : thrust coefficient
- C_P : power coefficient
- ρ : density (kg/m^3)
- A_d : disc area (m^2)

1. Introduction

The growing worldwide demand for renewable energy, coupled with apparent pool of energy within the world's tidal currents, has led to considerable interest in tidal power development over the last 25 years. However, there is not yet been done any theory or method to analyze tidal power extraction in particular. And it is hard to benchmark the efficiency of a given tidal power device or scheme, and to optimize a design for full scale system subsequently [1].

Albert Betz (1885 - 1968), a German physicist and a pioneer of wind turbine technology, introduced a method to determine the limit power of extraction in a fluid. That is the "Actuator Disc Theory" (ADT), the method for characterization of an actual tidal turbine in a solution of Reynolds Averaged Navier-Stokes equations (RANS). An actuator disc is a region where similar forces are applied to a flow as would be imposed by an actual turbine. The application of the model in an

† Corresponding Author (Dept. of Marine System Engineering, Mokpo National Maritime University, E-mail: cjyang@mmu.ac.kr, Tel: (061)240-7085)
1 Graduate school, Mokpo National Maritime University
2 Division of Mechanical and Information Engineering, Korea Maritime University

This paper is extended and updated from the short version that apeared in the Proceedings of the International symposium on Marine Engineering and Technology (ISMT 2011), held at BEXCO, Busan, Korea on October 25-28, 2011.

infinite volume of air is used in the analysis and design of wind turbines. Since the flow of air in the atmosphere is different to that of a liquid constrained in an open channel due to the air's negligible density, ADT can be applied for tidal turbines with some modification and extra consideration. ADT play an important role in study of multi-turbine array operation, especially in CFD simulation. ADT helps save time and computer power since such complicated model as turbine is replaced by a simple shape that more convenient for analysis.

In this paper, ADT is applied to a flow field consisting of two tidal turbines positioned longitudinally. All simulations are carried out in the same flow field, only the longitudinal space between two turbines is regulated to analysis and compare wake effects.

2. Methodology

2.1 Actuator Disc Theory

In this one-dimensional actuator disc model, the turbine rotor is represented by an "actuator disc" through which the static pressure has a jump discontinuity (Figure 1). A control volume fixed in

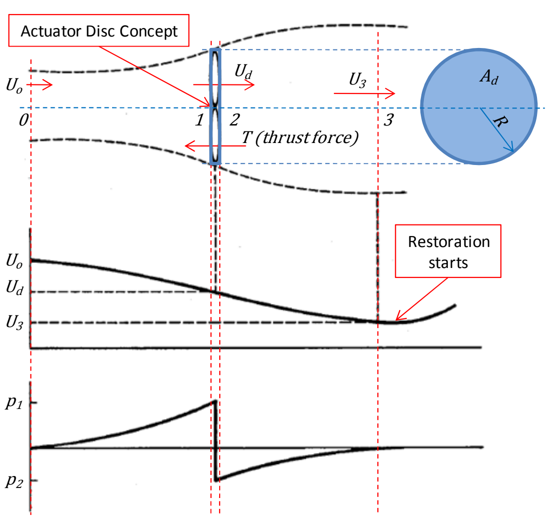

Figure 1: Actuator disc theory

space whose external boundary is the surface of a stream tube is considered. The fluid passes through the rotor disc, a cross-section of the stream tube upwind of the rotor, and a cross-section of the stream tube downwind of the rotor.

Since fluid does not pass through the stream tube porting of the control volume boundary by definition of a stream tube, applying the conservation of mass (which asserts that the instantaneous rate of change of mass within a control volume must be equal to the net flux of mass out of the control volume) to the control volume gives:

$$U_o A_o = U_1 A_1 = U_2 A_2 = U_3 A_3 = U_d A_d \tag{1}$$

where U_d is the velocity at disc and A_d is the cross section area of the disc.

The thrust at the rotor disc, T, can be found by applying the conservation of linear momentum to the control volume in the axial direction. This results in:

$$T = \rho A_o U_o^2 - \rho A_3 U_3^2 \tag{2}$$

But since $A_d = A_1 = A_2$, we have $U = U_1 = U_2$, Equadion (2) can be rewrite as:

$$T = \rho A_d U_d (U_o - U_3) = (P_1 - P_2) A_d \tag{3}$$

Since no work is done on either side of the disc, Bernoulli's equation can be applied to obtain the pressure incorporated into Equation (3):

$$\begin{aligned} P_o + \frac{1}{2}\rho U_o^{\,2} &= P_1 + \frac{1}{2}\rho U_d^2 \\ &= P_2 + \frac{1}{2}\rho U_d^2 = P_3 + \frac{1}{2}\rho U_3^{\,2} \end{aligned} \tag{4}$$

By equating Equations (3) and (4), the velocity of the flow through the rotor disc is the average of the upwind and downwind velocities:

$$U_d = \frac{U_o + U_3}{2} \quad (5)$$

An axial induction (sometimes called interference) factor, a, is defined as the fractional decrease in wind velocity between the free stream (upwind) and the rotor plane:

$$a = 1 - \frac{U_d}{U_o} \quad (6)$$

As a increases from zero, the downwind flow speed steadily decreases until, a = 1/2, meaning that the rotor has completely stopped and the simple theory is no longer applicable.

From Equation (3) and (5) we have:

$$T = \frac{1}{2}\rho A_d U_o^2 4a(1-a) \quad (7)$$

Hence, to demonstrate a turbine's induction rate, the dimensionless thrust coefficient, C_T, is defined as:

$$C_T = \frac{T}{\frac{1}{2}\rho A_d U_o^2} = 4a(1-a) \quad (8)$$

From the definition of power absorbed at turbine disc:

$$\text{Power} = T.U_d = T.U_o(1-a) = \frac{1}{2}\rho A_d U_o^3 4a(1-a)^2 \quad (9)$$

Another coefficient, power coefficient C_P is defined as:

$$C_P = 4a(1-a)^2 \quad (10)$$

It is simple to evaluate that C_P reaches maximum at a = 1/3. C_{Pmax} = 16/27 ≈ 59.3% and this is well-known as the Betz limit of power efficiency for wind turbines as well as tidal turbines [2].

2.2 CFD Modeling

The calculation domain is shown on Figure 2.

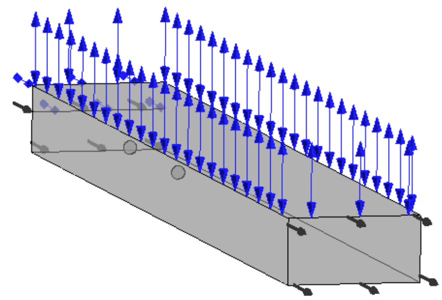

Figure 2: Calculation domain.

Table 1: Initial Calculation Circumstance.

Parameters	Values
Domain size:	8m(L)x1m(W)x0.5m(H)
Disc diameter:	0.1m
Disc thickness:	0.004m
Froude number:	0.175
Reynolds number:	3.5e4
Inflow velocity:	$U_o = 0.3\left(\frac{y}{0.15}\right)^{\frac{1}{10}}$ (m/s)
Mean Inflow velocity:	U_o = 0.3 (m/s)
Induction factor:	a = 0.33
Thrust coefficient:	C_T = 0.89

Initial input parameters are listed in Table 1. This calculation domain is made for a scale scenario with Froude number, Fr = 0.175. Thus, it is corresponded to an actual model of 10 m turbine in a 30 m water depth channel with mean inflow velocity of 3 m/s. Typical value of Froude number for full scale channels are within 0.1 - 0.2, and value less than 0.5 generally ensure stable flow when there are no obstacles in water column [3].

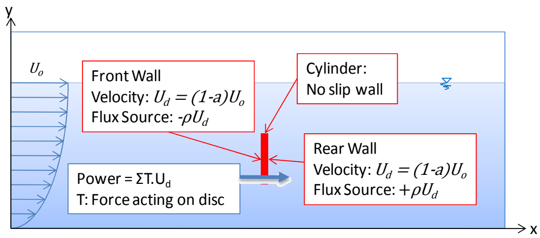

Figure 3: Disc as turbine rotor definition.

Boundary conditions are set up as:

Inlet: Cartesian normal speed. Since the flow is affected by seabed surface roughness, the velocity has gradient characteristic as shown in Figure 3. Many studies have found this velocity profile can be defined by several power laws as $1/7^{th}$ power law, $1/10^{th}$ power law and logarithm power law [3-5]. In this study $1/10^{th}$ power law velocity profile is selected for most calculations. Initial water level is set to 0.3m.

Outlet: Static pressure.

Sidewall: Free slip wall boundary.

Bed plane: As real sea bed is rough surface. So non-slip wall is defined for this boundary.

Opening: Air opening.

Disc front and rear walls: Free slip walls with flux sources (Figure 3).

Disc cylinder: Free slip wall.

Free surface: Volume of fluid (VOF) model.

Simulation is done in steady state. Turbulence model k-ε is used since it is the most commonly used of all the turbulence models in CFD [6]. For steady state calculations, max integration is set to 4000 to ensure convergence with convergence criteria of 1e-5.

2.3 Mesh Independence Study

A structured hexa-mesh was generated at different quality in term of node number. Table 2 shows the meshes made so far for all calculations done in this paper, for both single turbine case and two turbines array.

Table 2: Number of node for different meshes.

Mesh Density	1 Disc	2 Discs
Coarse	120,000	300,000
Medium	530,000	800,000
Fine	940,000	1,500,000

The meshes were considered as coarse mesh, medium mesh and fine mesh.

Figure 4 and Figure 5 in turn show the mesh formation and calculation results on single turbine flow field.

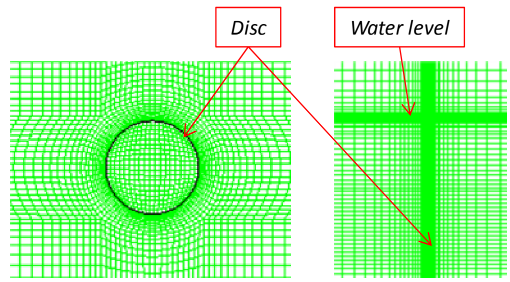

Figure 4: Medium mesh formation.

As shown in Figure 5, mesh quality provided different results. The coarse mesh presents a linear-like trend of velocity deficit at far wake, while the rest present higher order curves and somewhat is more accurate.

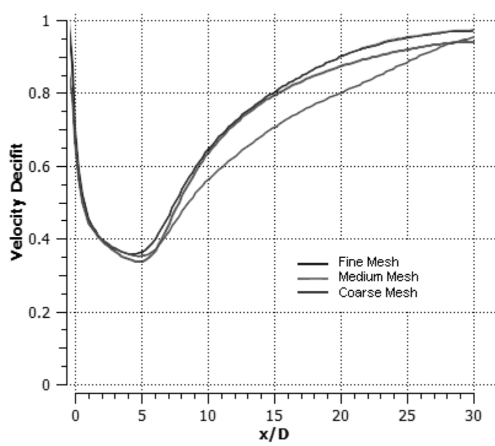

Figure 5: Single turbine centerline velocity deficit for different mesh qualities.

Medium mesh size is able to provide accurate results while requiring less computer power and saving more time in comparison to fine mesh. Thus, most of the simulation data presented here is extracted from medium mesh calculations.

3. Results and Discussion

3.1 Single Turbine

Effect of inflow velocity was tested on single turbine domain. As mentioned above, three power laws were applied to the inflow velocity (Figure 6).

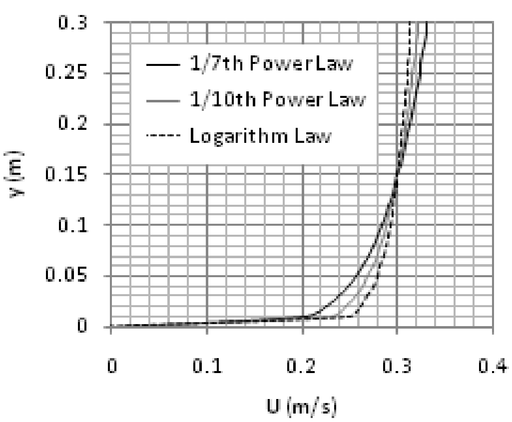

Figure 6: Inflow velocity profile definition.

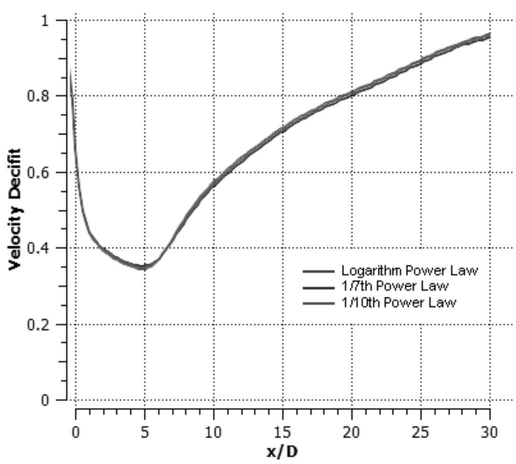

Figure 7: Single turbine centerline velocity deficit for different inflow velocity profiles.

The first three calculations at different inflow velocity profiles are done on a domain of half length (maximum downstream location is 35D). The turbine disc is characterized by C_T of 0.84 (a = 0.2). Figure 7 shows the velocity deficit along the centerline of the disc. All the parameters are presented in dimensionless view.

As calculated from CFD-Post, in three cases the turbine disc shows similar performance when it absorbed about 44% of stream power and reaches maximum restoration of approximately 0.9 at 35D.

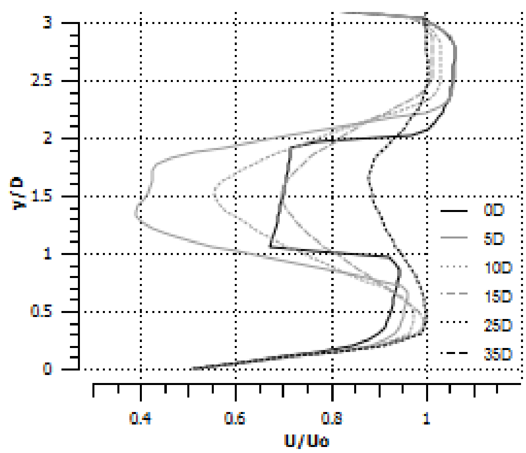

Figure 8: Far wake profiles as resulted from applying 1/10th power law inflow velocity.

Many researches and studies have already conducted with 1/7th and logarithm power laws. Hence, this paper put interest in 1/10th power law for comparison. However, the graph shows no significant difference among three curves. The far wake velocity profile of1/10th power law is shown in Figure 8. This is similar to Bahaj's work in his recent studies [3].

Since 35D seems not long enough to predict the full restoration, the next simulation is done on a flow field of 70D downstream length, this is also the flow field for all two turbines array simulations. Calculation data are shown in Figure

9 and Figure 10.

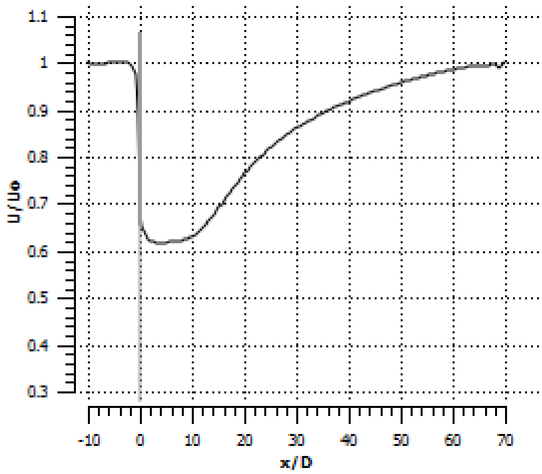

Figure 9: Centerline velocity deficit for as far as 70D downstream location.

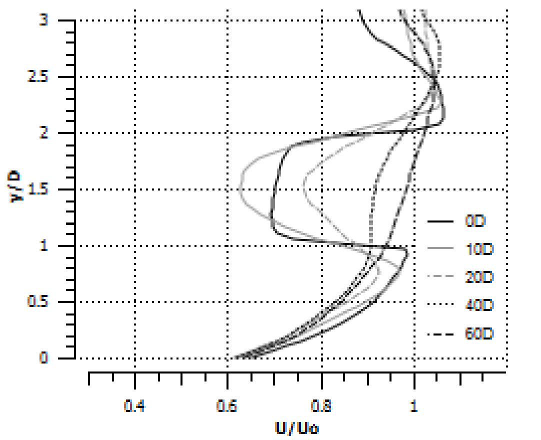

Figure 10: Far wake profiles for as far as 70D downstream location.

In this case, turbine disc is characterized by C_T of 0.89 (a = 0.33), this will result in maximum power efficiency theoretically. Inflow velocity is kept as 1/10th power law.

The deficit in Figure 9 shows a full restoration at around 65D-70D, but calculated C_P is 49.83%. Another far wake characteristics illustration in Figure 10 shows almost full restoration at disc center (y/D = 1.5) at 60D.

3.2 Two-turbine Longitudinal Array

Based on the evaluation of single turbine operating performance, simulations for two turbines positioned longitudinally were conducted with the same calculating circumstance. Totally five simulations are done for five cases of longitudinal space between turbines: 15D, 20D, 25D, 30D and 35D. Figure 11 shows the centerline deficit and Figure 12 shows the far wake profiles of these five simulation results.

It is clearly shown that no 100% restoration point existed in Figure 11. This is reasonable since conclusion from single case calculation has stated that at least 70D downstream distance should be provide in order to predict the full restoration. Even for the 15D case, the downstream length for 2nd turbine is as far as 55D, but maximum restoration only reaches 0.92 at 67D (corresponds to 52D for single turbine calculation domain). Stream energy is unable to fully restore in every cases. As a consequence, the second stage of absorption at the 2nd turbine is not as efficient as the first one.

In Figure 12, there is some disturbance of flow at 70D, this is additional effect at outlet boundary during computational solving process and has no abnormal change to the results. The far wake velocity profiles show smooth gradient with reasonable pattern comparing to actual flow and other recent studies. Energy extraction rate of the first turbine maintained almost constantly regardless of change in the second turbine's position. Opposite, the far wake from 2nd turbine location downward has much influenced by upstream flow.

In summary, data collected from simulations were put in Table 3.

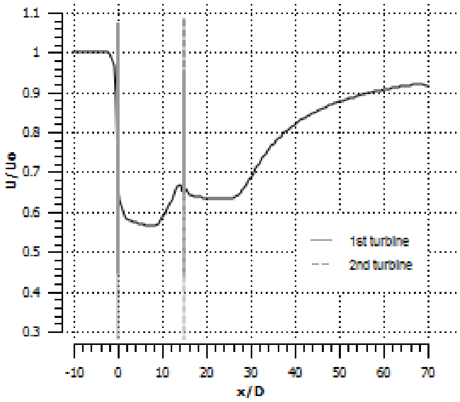

(a) 15D

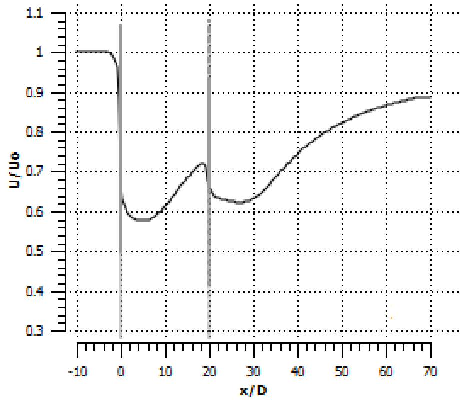

(b) 20D

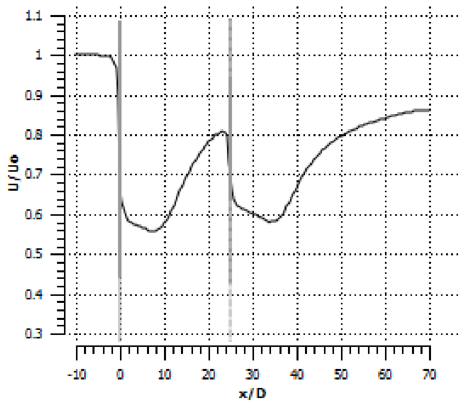

(c) 25D

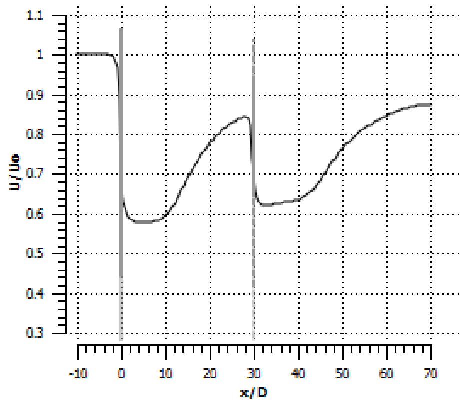

(d) 30D

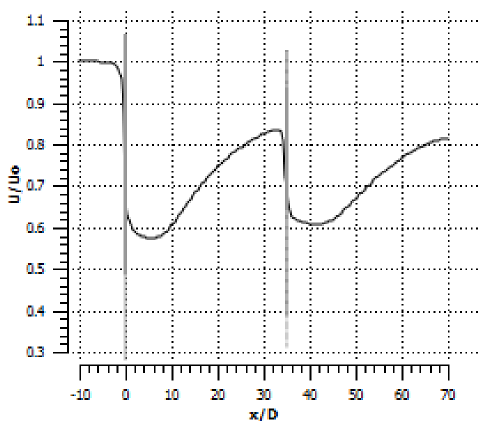

(e) 35D

Figure 11: Two turbines array centerline velocity deficit at different longitudinal spaces.

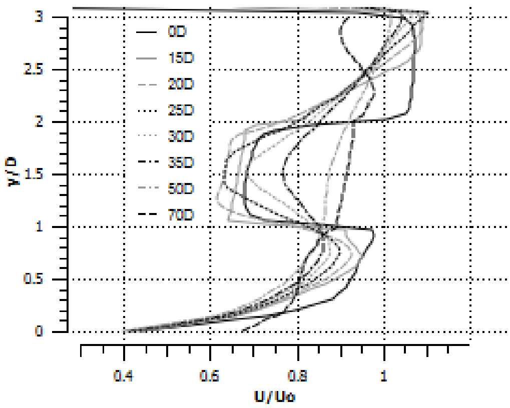

(a) 15D

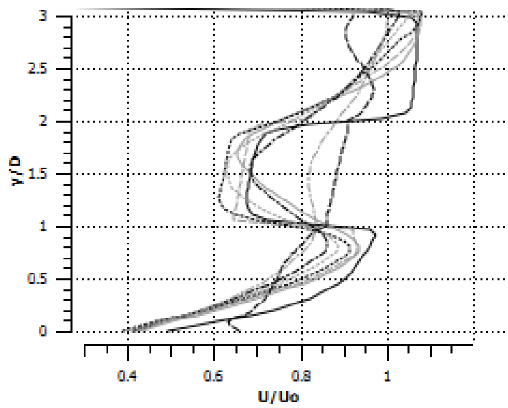

(b) 20D

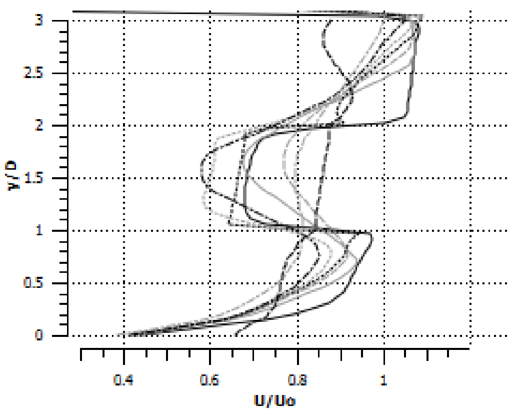

(c) 25D

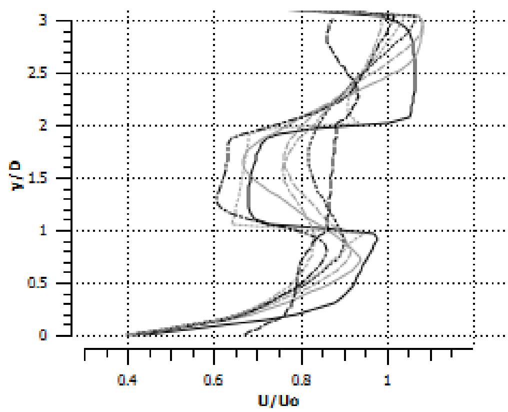

(d) 30D

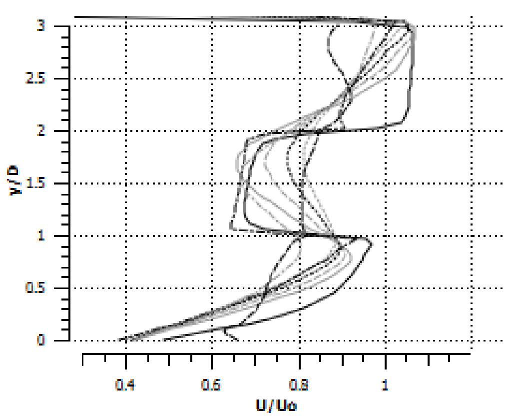

(e) 35D

Figure 12: Two turbines array far wake profiles at different longitudinal spaces.

Table 3: Two turbines array far wake evaluation data.

Space	15D	20D	25D	30D	35D
1st turbine absorption (%)	50.07	50.1	49.98	50.93	52.21
1st turbine max restoration (location)	0.67 (14D)	0.72 (19D)	0.81 (24D)	0.84 (28D)	0.84 (33D)
2nd turbine absorption (%)	15.75	19.0	26.05	29.51	37.77
2nd turbine max restoration (location)	0.92 (67D)	0.89 (69D)	0.86 (68D)	0.87 (68D)	0.81 (69D)

4. Conclusion

This paper introduces an approach of RANS actuator disc theory for tidal current turbine analysis using CFD and extends the study to two turbines longitudinal array calculation. CFD simulation based on actuator disc theory is conducted on both single and two turbines cases. To sum up, the following conclusions are given.

1) The results showed very little effect of inflow velocity profiles to the far wake of flow. For single turbine, at maximum power efficiency given in advance, 100% restoration is found at 65D-70D downstream location, and power extraction rate is 49.83%.

2) For two longitudinally positioned turbines in the same flow field, full restoration is not capable for both turbines. The 1st turbine's performance is mostly maintained and similar to that of single turbine with almost unchanged power coefficient for different longitudinal spaces. However, CFD calculated C_P is not as high as stated in theory.

3) Due to change in upstream velocity profiles, the second turbine's performance is always lower than the first one. Longer distance should be put in consideration to ensure full restoration before the second extraction stage.

Most of simulations in this paper are calculated at theoretical maximum turbine performance. Plus, mean inflow velocity of 3 m/s (full scale parameter) is claimed to be high. Thus, it is reasonable for such far predicted restoration. Slower inflow velocities, smaller induction factors. Other influence factors therefore should be investigated. These are the next topics for future discussions and studies.

Acknowlegements

This research is financially supported by The Ministry of Knowledge Economy of Korea through New & Renewable Energy R&D Program (20093021070010) and RIS Project(Invigoration of green marine equipment for new growth, project No. B0012286).

References

[1] G. T. Houlsby, S. Draper and M. L. G. Oldfield, Application of Linear Momentum Actuator Disc Theory to Open Channel Flow", University of Oxford, Department of Engineering Science, Report No. OUEL 2296/08, 2008.

[2] T. Burton, D. Sharpe, N. Jenkins, E. Bossanyi, Wind Energy Handbook, Wiley, 2001.

[3] M. E. Harrison, W. M. J. Batten, L. E. Myers and A. S. Bahaj, "Comparison between CFD simulations and experiments for predicting the far wake of horizontal axis tidal turbines", Renewable Power Generation, 2010, vol. 4, pp. 613-627, 2009.

[4] L. Bai, R. R. G. Spence and G. Dudziak, "Investigation of the influence of array arrangement and spacing on tidal energy converter (TEC) performance using a 3-Dimentional CFD model", Proceedings of the 8th European Wave and Tidal Energy Conference, Uppsala, Sweden, 2009.

[5] Carbon Trust, "Tidal streams and tidal stream energy device design", 2006.

[6] W. Graebel, Advanced Fluid Mechanics, Academic Press, 2007.

Author Profile

Chang-Jo Yang

He received his B.E. and M.E. degrees from Korea Maritime University, and his Ph.D. from Kyushu Institute of Technology. He is currently a professor in the Dept. of Marine System Engineering at Mokpo National Maritime University. His research interests include fluid machinery, flow visualization and CFD.

Anh Dung Hoang

He received his B.E. from Vietnam Maritime University. He is studying master course at Mokpo National Maritime University. His research interests include fluid machinery, CFD and thermodynamics.

Young Ho Lee

He received his B. Eng. and M. Eng. degree form Korea Maritime University, and his Dr. Eng. form the University of Tokyo, Japan. He is currently a professor in the Division of Mechanical and Information Engineering, Korea Maritime University. His research interests are renewable energy such as wind, micro-hydro & marine (wave & tidal stream) to optimize runner blade design by CFD & PIV. He is now vice-president of Korea Wind Energy Association, Korea Fluid Machinery Association and Korean Society for New & Renewable Energy.